Numerical simulation of Heat Transfer Enhancement in A channel Flow by Rectangular Winglet Vortex Generator

El hassen A. A. Omer and Mona Y. Alshibani
Department of Aeronautical Engineering, Faculty of Engineering, University of Tripoli

Abstract

A numerical simulation was performed to investigate the effects of longitudinal vortices on the heat transfer enhancement of a laminar flow in a rectangle duct mounted with rectangular winglet pair on the bottom wall. A CFD ANSYS Fluent software was used to compute the 3-D steady viscous flows with heat transfer. The effects of Reynolds number ranging from 250 to 2000, winglet heights and different attack angles of the vortex generators were studied. The comparisons of the fluid flow and heat transfer characteristics for the cases with and without rectangular winglet pair were carried out using parameters such as the Nusselt number, the friction coefficient and performance evaluation criteria PEC to gauge the overall efficiency of the system. Results show that mounting rectangular winglet pair on a channel flow can significantly enhance heat transfer. The distributions of secondary flow on the cross sections are consistent with the distributions of Nu and f for different attack angles. The results show that there is a 11 - 29% increase in the Nusselt number for channels with LVGs, while the friction factor increased by 19 - 30%, causing the overall PEC to increase by 4 - 18%, for the studied range of Reynolds number. Under constant geometrical parameters, the Nu and pressure drop increased as the height of the RWP increased. The maximum heat transfer performance is obtained when the attack angle is 30° due to the maximum value of secondary flow generated by rectangular winglet pair.

Keywords : rectangular winglet, vortex generator, heat transfer enhancement, pressure drop, numerical simulation

Nomenclature

A	Area, m^2.	T	Temperature, K
Cp	Specific heat, J/kg.K	u	Velocity components
D_h	Hydraulic diameter, m.	VG	Vortex generator
DP	Pressure drop, Pa.	x	Axial distance, m
f	Friction factor.	α	Roll angle
h	Heat transfer coefficient, W/m^2 K.	β	Angle of attack
H	Test section height, m.	μ	Viscosity, kg/ms
k	Thermal conductivity, W/m.K	ρ	Density, kg/m3
L	Channel length, m	Λ	Aspect ratio
LV	Longitudinal vortex		
Nu	Nusslet number	Subscripts	
p	Pressure, N/m^2	0	Channel without VG
PEC	Performance evaluation criteria	b	Bulk
Pr	Prandtl number	in	Inlet
Re	Reynolds number	m	mean
RWP	Rectangular winglet pair	x	Local
S	Surface area m^2		

1. Introduction

The high performance thermal systems are needed in many industrial applications such as shell-and-tube type heat exchangers, automotive industry, electric circuit in electronic chip cooling, air conditioning and refrigerant applications, internal cooling of gas turbine blades and aerospace industry. Hence, several methods to improve heat transfer in the systems have been developed extensively with a view to reducing the size, weight and cost of the heat exchanger systems.

In general, techniques for increasing heat transfer are classified into three main categories, namely active, passive, and combined methods. The active method requires outside energy but is quite complex. The passive method does not require external energy, it requires modifying the surface and geometry of a channel. Passive methods are more widely used than active methods because they are economical and easy to produce, when two methods or more combined for heat transfer enhancement, it is called combined methods [1]. One of passive techniques for convective heat transfer enhancement can be achieved by generating secondary flow structures that are added to the main flow to intensify the fluid exchange between hot and cold regions in the system. One method involves the use of vortex generators to produce streamwise and transverse vortices on the top of the main flow. These vortices disrupt the growth of the thermal boundary layer and enhances heat transfer rate. There are two types of vortex generators; transverse vortex generators (TVGs) when the axis of vortices is perpendicular to the fluid flow, and longitudinal vortex generators (LVGs) when the axis of the vortices is parallel to the fluid flow. Both types can be applied within channels to extend the surface area and generate vortices to enhance the heat transfer. Studies have reported that better heat transfer enhancement is achieved using LVGs compared to TVGs [2].

Several experimental and numerical investigations were conducted to study the heat transfer enhancement downstream from vortex generators. Syaiful et al. [3] studied numerically and experimentally, the strength of the vortex generated by VGs by trying to reduce the pressure drop in the flow by using concave rectangular vortex generator in a channel flow. The study results indicate that the observed heat transfer coefficients from the experimental and simulation results have a similar tendency with relatively small errors. A reduction in pressure drop is observed with the use of perforated concave rectangular winglets the nonperforated ones although there was a slight decrease in heat transfer improvements. Li et al. [4] considered the effect of increased pressure drop on pumping power to improve heat transfer by mounting a delta winglet vortex generator around the tube. The thermal-hydraulic performance found by them was improved by installing VG around the tubes of the fin and tube heat exchanger. Salleh et al. [5] investigated experimentally and numerically the thermal-hydraulic performance of fluid flow that passes through the fin and tube heat exchanger with and without using a trapezoidal winglet vortex generator. The experimental results showed that heat transfer could be increased by variations in geometry, installation configuration, aspect ratio (Λ), and specific angle of attack (β). Meanwhile, numerical simulation results illustrated that flat trapezoidal winglets mounted with a common flow-up orientation at $\Lambda = 3$ and $\beta = 10\ ^\circ$ have the best thermal-hydraulic performance. This performance is found based on increased heat transfer and decreased pressure drop. Song et al. [6] conducted a numerical study to determine the characteristics of heat transfer with the use of concave and convex curved vortex generators in channels in the laminar flow. Their results showed that concave curved VG could improve heat transfer better than curved convex VG and plain VG. Concave curved VG has a higher JF value at $Re = 1400$, $\beta = 20\ ^\circ$, and $\theta = 80\ ^\circ$, which is 11.3% compared to that of convex curved VG.

Wijayanta et al. [7] studied heat transfer enhancement of internal flow by inserting punched delta winglet vortex generators with various attack angles. Their results revealed that the punched delta winglet vortex generators in a tube provided considerably higher heat transfer coefficient than the tube without the insert through pressure loss was also increased.
Sinha et al. [8] investigated enhancement of heat transfer in a fin-tube heat exchanger using rectangular winglet type vortex generators. They found that significant improvement in the heat transfer performance due to the nozzle-like flow passages created by the winglet pair and the region behind the circular tube which promote accelerating flow. Aliabadi et al. [9] studied performance of a plate fin heat exchanger with vortex-generator channels. They found that heat transfer coefficient and pressure drop values enhance as the wings height, longitudinal wings pitch, and transverse wings pitch decrease and the wings width, channel length, and wings attack angle increase. Delac et al. [10] investigated the heat transfer enhancement in a fin and tube heat exchanger using vortex generators. They found that in Laminar flow conditions, the variation of winglet size and angle of attack can result in the increase of heat transfer but with a penalty of pressure drop. He et al. [11], investigated the heat transfer enhancement and pressure loss penalty for fin-and tube heat exchangers with rectangular winglet pairs (RWPs) were numerically investigated in a relatively low Reynolds number flow. The purpose of this study was to explore the fundamental mechanism between the local flow structure and the heat transfer augmentation. The numerical study involved three dimensional flow and conjugate heat transfer in the computational domain, which was set up to model the entire flow channel in the air flow direction. The effects of attack angle of RWPs, row-number of RWPs and placement of RWPs on the heat transfer characteristics and flow structure were examined in detail. It was observed that the longitudinal vortices caused by RWPs and the impingement of RWPs directed flow on the downstream tube were important reasons of heat transfer enhancement for fin-and-tube heat exchangers with RWPs.

Based on this literature study, VG can increase heat transfer by generating vortices that enhance fluid mixing. However, this improvement in heat transfer is accompanied by an increase in flow resistance, resulting in high pumping power. Therefore, the optimization of thermal-hydraulic performance has become a concern of many researchers recently. Therefore, the present study focuses on a detailed analysis relating the flow pattern through VG to the increase in its heat transfer rate and pressure drop associated with it in a channel flow with RWP mounted in the bottom wall under laminar conditions. The effects of Reynolds number, the height of rectangular winglet pair (RWP), and the attack angle are investigated using numerical method.

2. Problem Formulation

The numerical model for fluid flow and heat transfer in the rectangular channel was developed under the following assumptions:

- Steady three-dimensional fluid flow and heat transfer.
- The flow is laminar and incompressible.
- Constant fluid properties.
- Body forces and viscous dissipation are ignored.
- Negligible radiation heat transfer.

Based on the above assumptions, the compact forms of the governing equations in physical space applied in this modeling are as follows, [12] :

Continue equation

$$\frac{\partial(\rho u_i)}{\partial x_i} = 0 \qquad (1)$$

Momentum equation

$$\frac{\partial(\rho u_i u_k)}{\partial x_i} = \frac{\partial}{\partial x_i}\left(\mu \frac{\partial u_k}{\partial x_i}\right) - \frac{\partial p}{\partial x_k} \quad (2)$$

Energy equation

$$\frac{\partial(\rho\, c_p u_i T)}{\partial x_i} = \frac{\partial}{\partial x_i}\left(k \frac{\partial T}{\partial x_i}\right) \quad (3)$$

The Reynolds number and the friction factor are defined as follows

$$Re = \frac{\rho u_{in} D_h}{\mu} \quad (4)$$

$$f = 2 \frac{\Delta p}{L} \frac{D_h}{\rho u_{in}^2} \quad (5)$$

The required pumping power to overcome pressure drop calculated by

$$RPP = u_{in} A \Delta p \quad (6)$$

In this case, since the flow is through a rectangular channel, the hydraulic diameter is

$$D_h = \frac{4A}{P} = \frac{2WH}{(W+H)} \quad (7)$$

The local Nu are determined by

$$Nu_x = \frac{h_x D_h}{k} \quad (8)$$

The local convective heat transfer coefficient is determined by

$$h_x = -k \frac{(\partial T/\partial n)}{T_w - T_b(x)} \quad (9)$$

where T_b is the bulk temperature of the heated surface side fluid and is defined as follows

$$T_b(x) = \frac{\iint u(x,y,z)T(x,y,z)dydz}{\iint u(x,y,z)dydz} \quad (10)$$

The mean heat transfer coefficient and Nu are determined as follows

$$Nu_m = \frac{h_m D_h}{k} \quad (11)$$

$$h_m = \frac{\int_S h_x\, dS}{\int_S dS} \quad (12)$$

A coefficient known as performance evaluation criteria (PEC) is used to simultaneously examine the increase in heat transfer and pressure drop. It is defined under the same pumping power as follows [13] :

$$PEC = \left(\frac{Nu}{Nu_0}\right) / \left(\frac{f}{f_0}\right)^{1/3} \quad (13)$$

Boundary conditions are required to solve governing equations. The boundary conditions defined in the computational domain are stated as follows;

Inlet upstream extended region:

$$u = u_{in}\ ,\ v = w = 0\ \ and\ T = T_{in} \quad (14)$$

Outlet downstream extended region

$$\frac{\partial u}{\partial x} = \frac{\partial v}{\partial x} = \frac{\partial w}{\partial x} = 0\ \ and\ \frac{\partial T}{\partial x} = 0 \quad (15)$$

Wall

$$u = v = w = 0\ \ and\ q = 0 \quad (16)$$

Hot wall

$$u = v = w = 0\ \ and\ T = T_w \quad (17)$$

Symmetry

$$w = 0\ , \frac{\partial u}{\partial z} = \frac{\partial v}{\partial z} = \frac{\partial T}{\partial z} = 0 \quad (18)$$

3. Numerical simulation

The dimensions of a rectangular channel on the computational domain of numerical simulation are 500 mm x 160 mm x 40 mm. While the dimensions of winglet are thickness is 0.002m, length is 0.04 m height is 0.02 m and winglet pair is 0.005 m apart from each other. The X-axis is the axis in the direction of flow, the Z-axis is the transverse axis of the flow, and the Y-axis is the distance between the upper wall and the lower wall. The computational domain of this numerical simulation is a control volume, which is half the volume of the geometry of a rectangular channel. An additional two regions, an inlet and an outlet extended regions of lengths of 400 mm and 600 mm respectively. The extended regions are required to ensure the fully developed flow at the entrance channel side, and there is no reverse flow in the exit side. The computational domain of this numerical simulation is shown in Fig. (1).

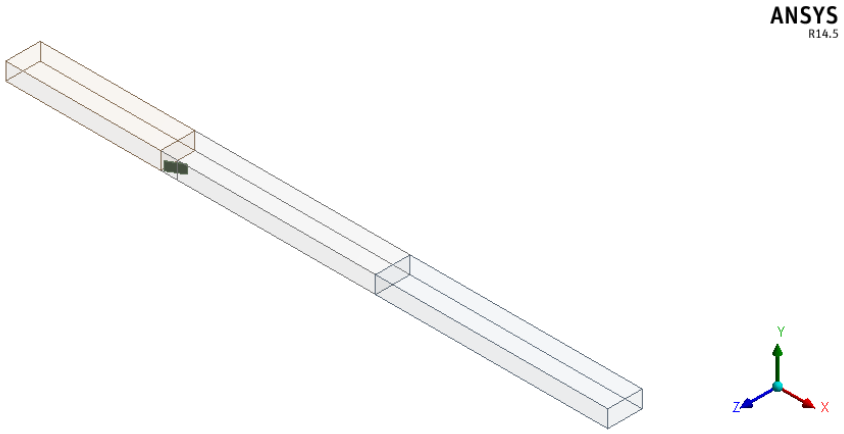

Fig. (1) Isometric view of the computational domains

Fig. (2) shows the grid formation in meshing. The simulation for 3D VGs on the rectangular flow channel, accuracy is needed in mesh generation to obtain good results in determining the velocity and temperature distribution. Mesh generation performed using just two types of meshing. Therefore, hexahedral coarser mesh was used in the upstream and downstream extended regions, while tetrahedral fine mesh was used for the tested region.

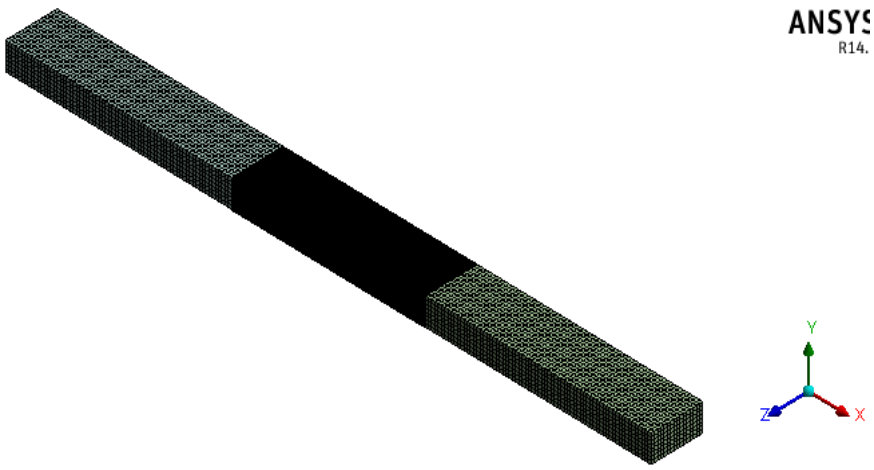

Fig. (2) Mesh layout

The governing equations were discretized by a second-order upwind scheme. SIMPLE algorithm used for pressure-velocity coupling. The viscous model was laminar. The residual convergence criteria were 10^{-5} for momentum and velocity, 10^{-8} for energy.
The fluid is air with a constant density of 1.225 kg/m³, dynamic viscosity of 1.7894E-5 kg/m·s, the constant pressure specific heat is 1006.43 J/m·K, and thermal conductivity is 0.0242 W/m·K. The inlet boundary has been given an inlet temperature of 300 K and velocity based on required Re. The pressure is assumed to be in atmospheric pressure in outlet boundary. The walls including the VG are in stationary state and no slip is applied to shear condition. For thermal conditions the walls are adiabatic and the heated wall constant temperature of 400 K is applied.

4. Mesh Sensitivity and Code Validation

A grid independence test was applied on a VG-enhanced channel to assess the density of mesh required. To determine the appropriate mesh density, all parametrs were kept constant and the solver is run with increasing mesh densities until no significant effect on the results is detected. The mesh independence testing is performed the mesh refinement is assessed by means of the global Nusselt number which is a major interest in our study. five meshes were used, Fig.(3) shows the average Nu calculated using each mesh. It is noticed that there is no significant difference in the computed results between the fourth and fifth grids. Hence, by a compromise between required accuracy and computation time, the fourth grid is selected for the simulations.

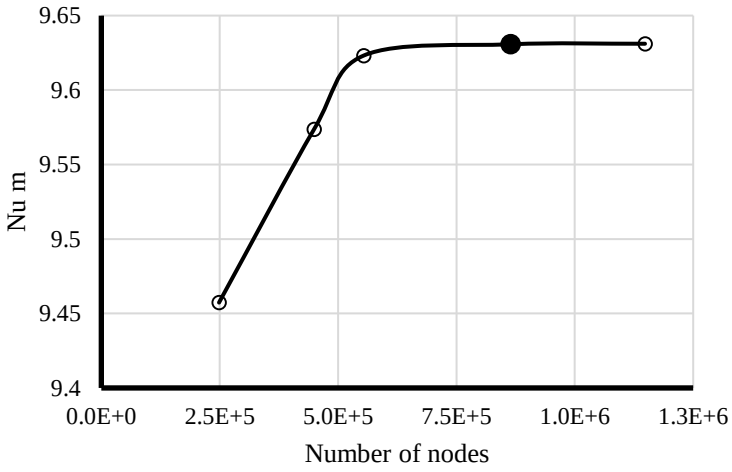

Fig. (3) Mesh independence testing,

Since the velocity and the temperature are set to be uniformed at the inlet of the omputational domain, it is considered that the flow is a developing flow. For thermally and hydraulically developing laminar air flow, the results are validated for Nusselt number using Stephan correlation [14]. The local Nusselt number is represented as followed:

$$Nu_x = 7.55 + \frac{0.024\ x_*^{-1.14}\left(0.0179\ Pr^{0.17}\ x_*^{-0.64} - 0.14\right)}{\left(1 + 0.0358\ Pr^{0.17}\ x_*^{-0.64}\right)^2} \quad (19)$$

Where :

$$x_* = x/\left(D_h Re\ Pr\right) \quad (20)$$

This correlation is valid in the range for Pr : 0.1 - 1000 for parallel plate channels with uniform wall temperature. The distribution of span-averaged Nusselt number calculated and compared with computational results obtained for smooth channel case. Fig. (4) represents the comparison between the correlation and the simulation results. It is found that the numerical results and experimental results are in good agreement, which indicates that numerical simulation program is reliable. The maximum percentage error is lower than 12 % and the average error is 5.9 % all along the tested channel.

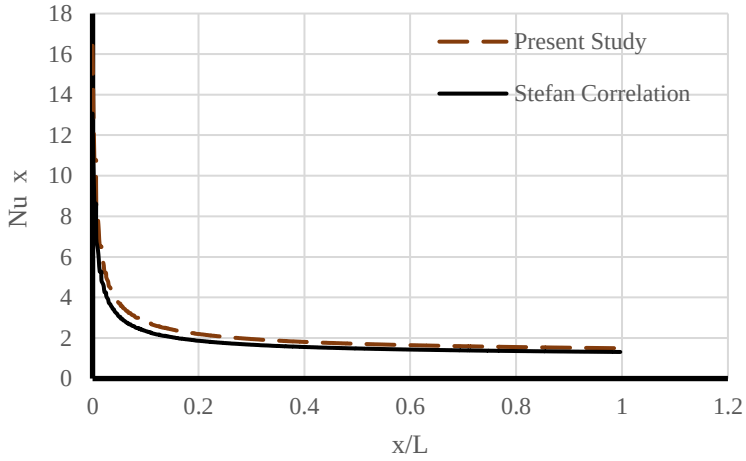

Fig. (4) Code validation

5. Results and Discussion

The numerical simulations are carried out for a rectangular channel with rectangular winglet vortex generator. The results of effects of varying Reynolds number, attack angles and winglet heights are analyzed in the following articles.

5.1. Effect of Reynolds number

The computations are performed for Reynolds number range (250 – 2000), while the winglet height, angle of attack β =30°.and roll angle α = 90° were constant. Fig. (5) shows the generation of secondary flow where a pair of longitudinal vortices with stronger strength is generated at the plane next to the trailing edge of RWP. Comparing the velocity distributions on the different cross-sections, the vortices pair in transverse direction is getting wider, while gradually decrease as they move in stream wise direction. Also, the velocity contors indicate that the intensity of induced vortices increase as the Reynolds number increased.

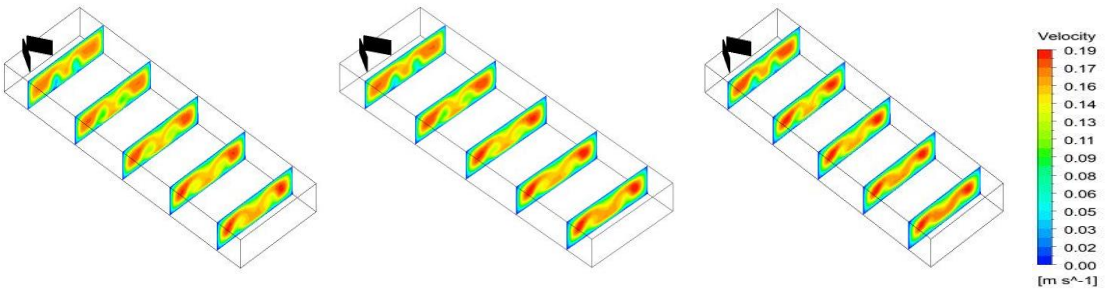

Re = 1500 Re = 1000 Re = 500

Fig. (5) Velocity contours at different axial sections

Fig. (6) shows the temperature profiles at the different cross-sections locations. It clearly shows that the longitudinal vortices lead to the deformation of the temperature profiles in the flow channel. This indicates that longitudinal vortices create a swirling flow which produces a better thermal mixing between the hot fluid near the wall and the cold fluid of core regions, and thus enhancing the heat transfer. Also, the plots indicating that the effect of the intensity of longitudinal vortices which increases as Reynolds number increased.

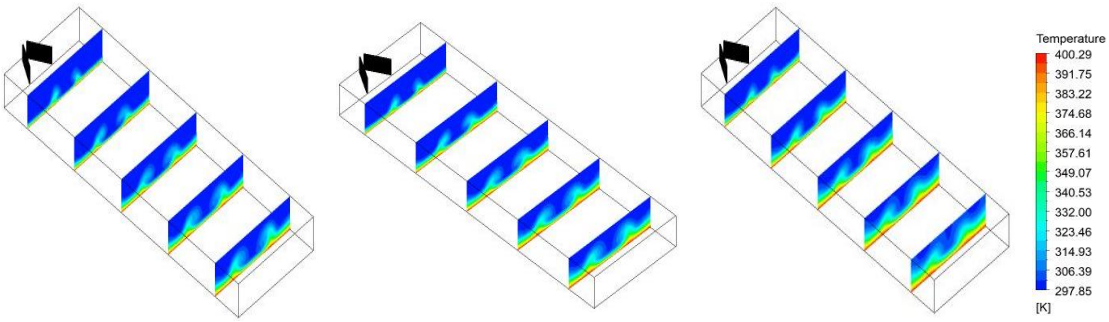

Re = 1500 Re = 1000 Re = 500

Fig. (6) Velocity contours at different axial sections

Fig. (7) display a comparison of the average Nu number for the flow channel with VG and smooth channel. Overall, the Nu increases with increasing Reynolds number. it is found that the use of RWP VGs increases the convection heat transfer, because RWP generates a longitudinal vortices which disturb, swirl and mix the fluid flow, hence, break the boundary layer developing and make it thinner, consequently enhancing the heat transfer.

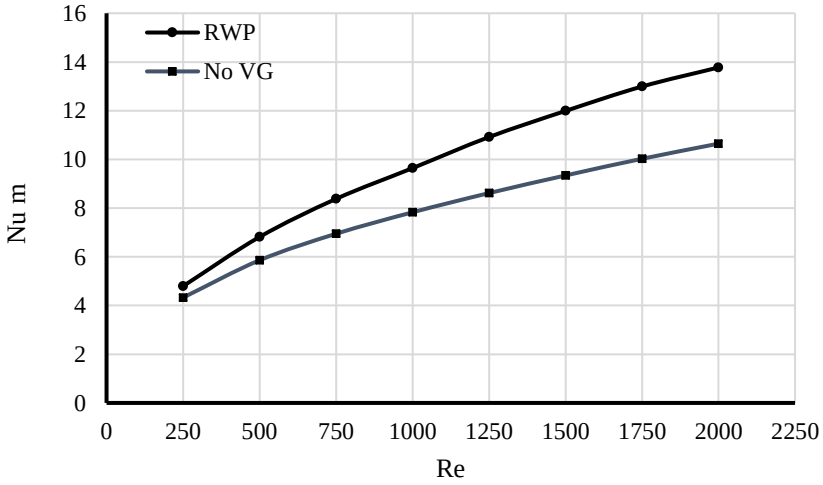

Fig. (7) Velocity contours at different axial sections

Fig. (8) represents the performance characteristics of installing the RWPVG in the channel, generally all the performance ratios more than one indicating that the VG enhancing heat transfer with increasing in the pressure drop.

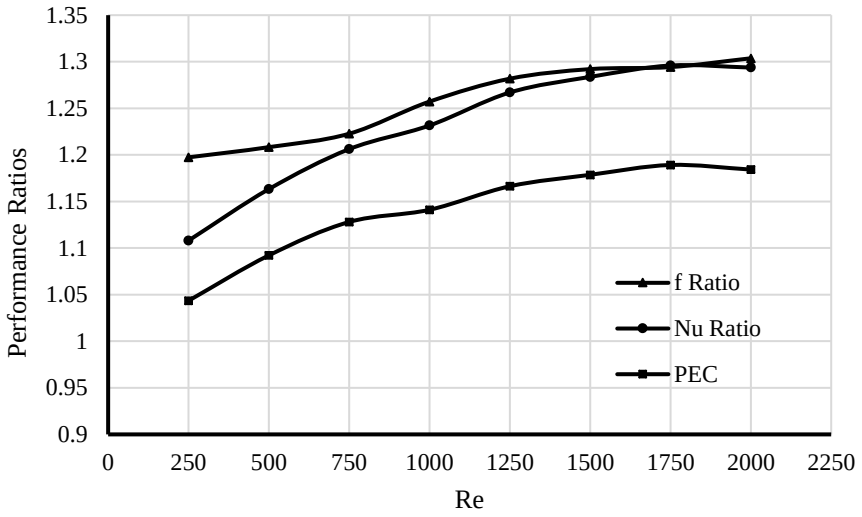

Fig. (8) Velocity contours at different axial sections

Fig. (9) shows a comparison of the pressure drop values between the channels with/without RWP vortex generator with variations in Reynolds numbers. It can be stated that the pressure drop of the results increase with increasing Reynolds numbers for both cases. In general, the installation of RWP in channel resulting a higher pressure drop due to formation of a vortex which caused a deviant flow from the main flow to yield in an increase in pressure drop.
When the pressure drop increases, the pumping power cost also increases, thereby increasing the operating cost, as shown in Fig. (9) which shows the required pumping power ratio as a function of Re. It is seen that higher pumping power is required at higher Reynolds numbers which can be explained due to increase in pressure loss across the channel with VG and higher flow rates. This increase in pressure drop increases the pumping cost. Therefore any augmentation device should optimize between the benefits due to the increased heat transfer coefficient and the higher cost involved because of the increased frictional losses.

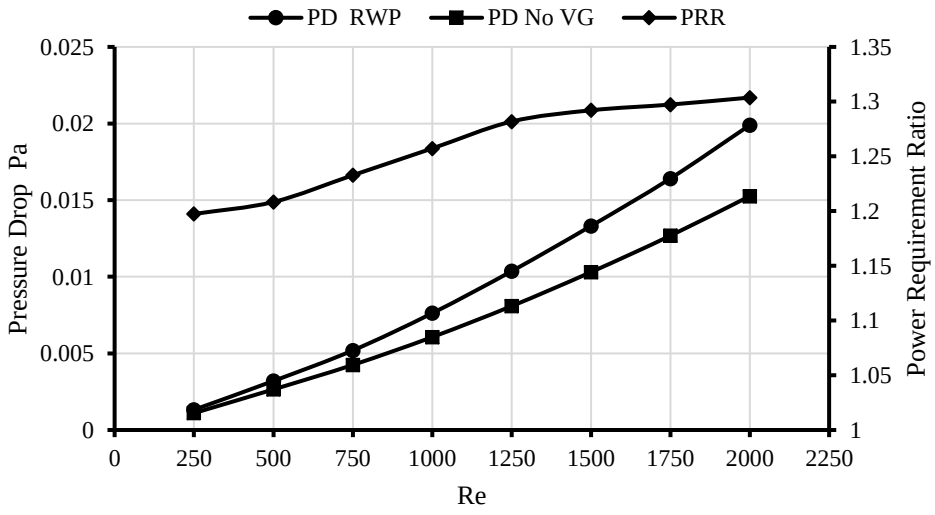

Fig. (9) Pressure drop and the required pumping power ratio

5.2. Effect of the height of RWP

The effects of the variation of height of RWP on heat transfer enhancement keeping the other parameters constant is analyzed here. At a fixed Reynolds number Re = 1000, Fig. (10) shows the plots of tangential velocity merged with temperature field at different planes along the stream wise direction and different RWP heights.

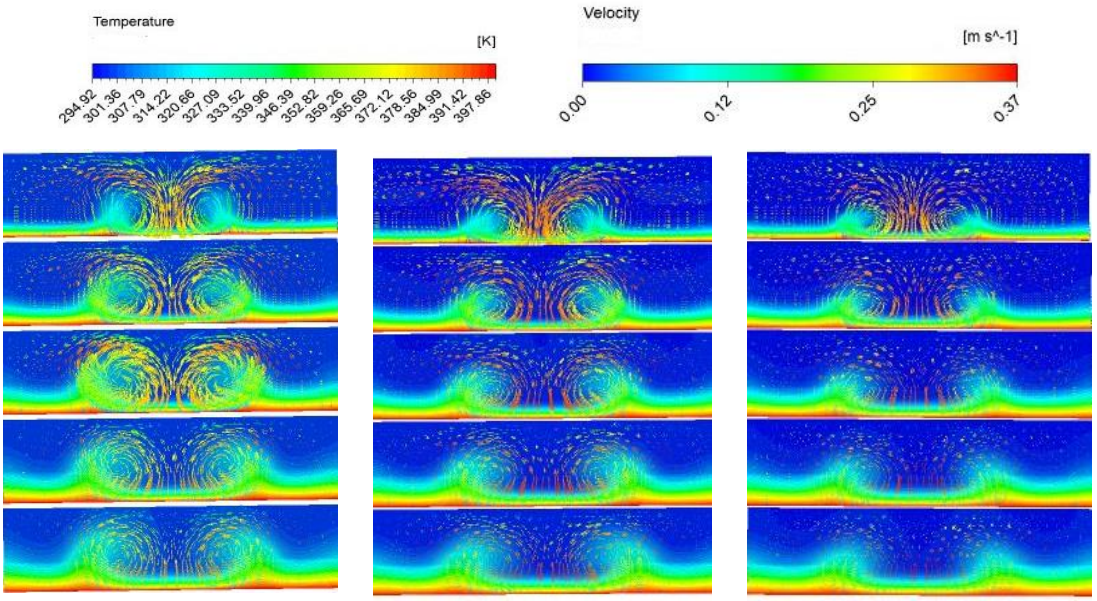

Fig. (10) Tangential velocity vectors with temperature contours at different axial sections

These plots indicate, generally that the vortices along the cross sections getting weaker where the vortices intensity decreases, and the intensity of longitudinal vortices decreases with the decrease in height of RWP. The effect of generated secondary flow clearly enhancing the heat transfer rates where the temperature distributions affected due to the vortex generator. These results consistent with the distributions of mean Nu shown in Fig. (11).

Figs. (11 and 12) show the increase of mean Nussult number and pressure drop with increasing the height of RWP for all the studied range of Re. This can be explained as when the height of the vortex generator increased, the projection area normal to the incoming flow increases causing an increase in the velocity at the side edge of the vortex generator for the same volume flow rate. Therefore the strength of the longitudinal vortices increases, leading to an increased heat transfer performance. In the same time, as the intensities of the longitudinal vortices increase their disturbances on flow are also stronger resulting in increasing the pressure drop. Therefore, heat transfer enhances with increasing RWP height, while pressure drop also increases with heights.

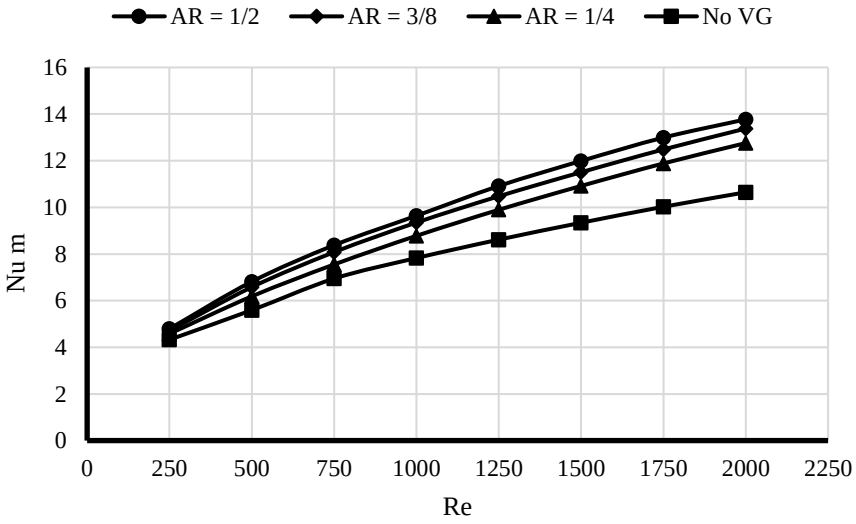

Fig. (11) The mean Nusslet number at different Reymolds numbers

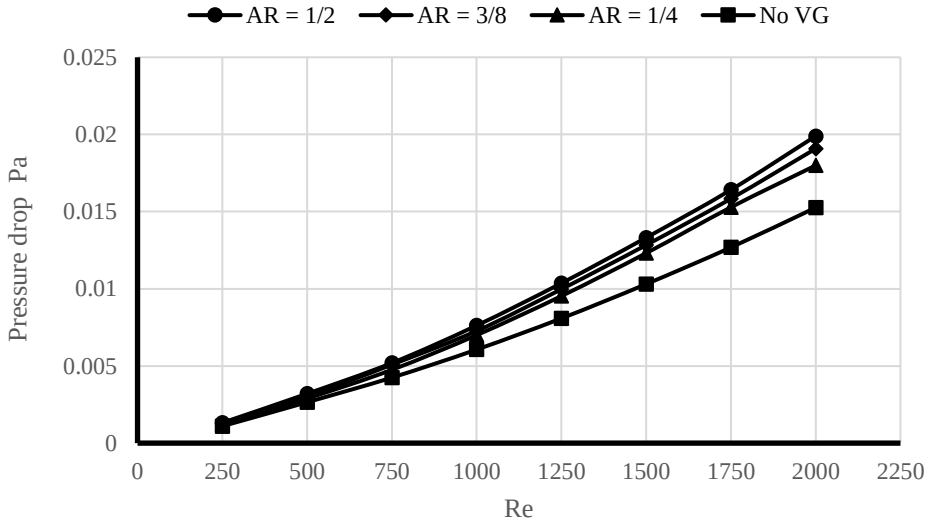

Fig. (12) The pressure drop along the test section at different Reymolds numbers

5.3. Effect of the angle of attack

A vortex generator with a fixed size and with various angles of attack are studied here. At a fixed Reynolds number Re = 500. Fig. (13) shows the tangential velocity fields under different attack angles of RWP at different locations in stream wise direction. The intensity of secondary flow on the cross sections changes along with the changing of attack angle of RWP, where the intensity of secondary flow with the increase in attack angle, when the attack angle changing from 15° to 30°. Then the intensity of secondary flow decreases with increase in the attack angle changing from 30° to 45°.

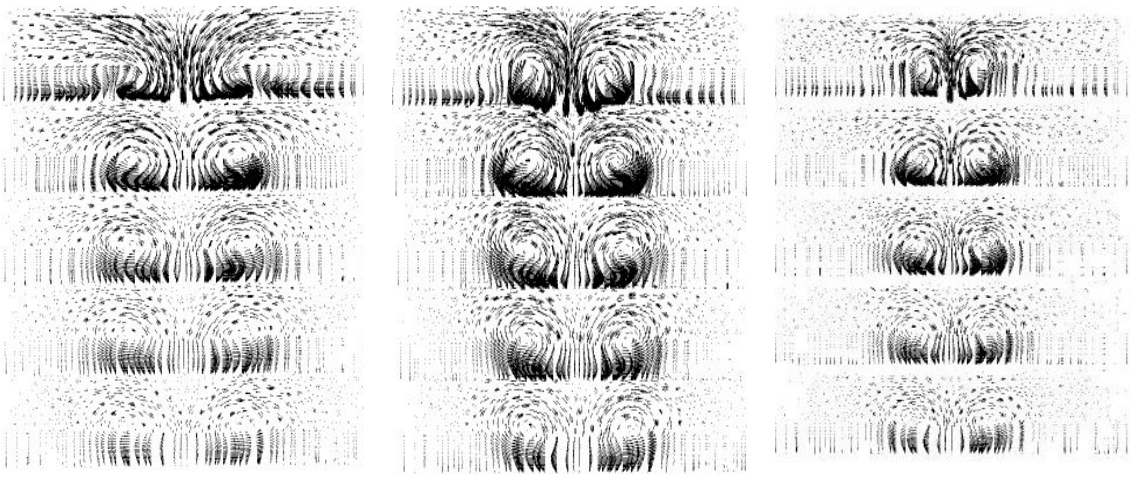

Fig. (13) Tangential velocity vectors at different cross sectional planes for different angles of attack

The maximum value of secondary flow intensity is obtained when attack angle is 30°. The distributions of secondary flow on the cross sections are consistent with the distributions of Nu and friction factor shown in Fig. (14). Thus, the best heat transfer performance obtained when the attack angle is 30° due to the maximum value of secondary flow generated by RWP. This is due to the fact that at higher angle of attack, the longitudinal component of generated vortices by the VG decreasesm there fore its effect on enhancing heat transfer and increasing pressure drop reduced.

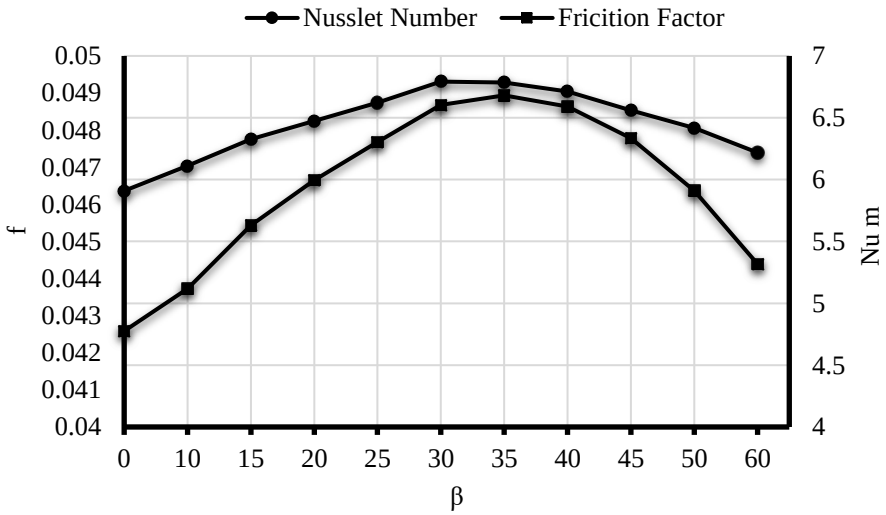

Fig. (14) the mean Nu number and friction factors for different angles of attack

Fig. (15) shows the effect of a RWP with different angles of attack on the performance ratios in a channel flow. The diagram shows for all cases the performance ratios are higher than the channel without vortex generator installed. And the vortex generator with an angle of attack of 30° brings about the highest performance.

Also, it can be noted that zero attack angle has approximately same friction factor as channel without vortex generator but a higher heat transfer, it can be explained as even though a vortex generator with a zero angle of attack does not generate any vortexes, it has a positive effect on heat transfer since it acts as a fin, increasing the heat transfer surface.

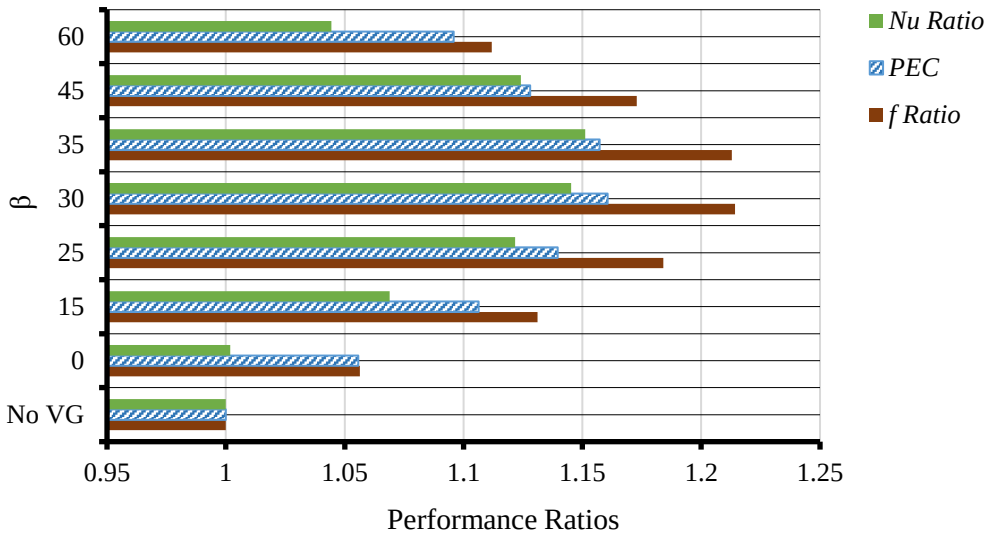

Fig. (15) Performance ratios presentation for different angles of attack

6. Conclusion

A numerical study of heat transfer enhancement by rectangular winglet type longitudinal vortex generator mounted on the bottom wall of the channel is investigated. The same model without RWP is also carried out for comparison. The effect of the height of RWP and the attack angle of RWP on the heat transfer and pressure drop are studied. Nusselt number, skin friction coefficient ratios and (PEC) are substantial factors that have been studied at laminar flow, the simulation results can be summarized as:

i. The performance of heat transfer can enhanced by mounting vortex generators on the surfaces of gas side. Vortex generators cause an augmentation in heat transfer of the channel over a plane channel for the same flow conditions.
ii. The longitudinal vortex generators significantly increase the circulation in the channel flow, the generated vortices by winglets changed the velocity and temperature distributions in channels. Hence enhancing the heat transfer.
iii. Nu highly increased with increasing of Reynolds number (Re), and an enhancement in the Nu obtained by using winglet inserts comparing with plane channel.
iv. The skin friction coefficient and pressure drop augment with the winglet inserts due to the increase of the resistance to the flow and formation of vortex flow.
v. Under constant geometrical parameters, the Nu and pressure drop increased as the height of the RWP increased.
vi. The maximum heat transfer performance is obtained when the attack angle is 30° due to the maximum PEC value and highest intensity of secondary flow generated by RWP.

References

[1]. Zhai, C.; Islam, M.D.; Simmons, R.; Barsoum, I.; Heat transfer augmentation in a circular tube with delta winglet vortex generator pairs, International Journal of Thermal Sciences 140, pp 480–490, (2019).

[2]. Wu, J.M. and Tao, W.Q; Numerical study on laminar convection heat transfer in a rectangular channel with longitudinal vortex generator. Part A: Verification of field synergy principle, International Journal of Heat and Mass Transfer, **51**(5–6): p. 1179-1191, (2008).

[3]. Syaiful, Hendraswari, M.P.; Utomo, T.S.; Soetanto, M.F.; Heat transfer enhancement inside rectangular channel by means of vortex generated by perforated concave rectangular winglets, Fluids, 6, 43, (2021).

[4]. Li, M.; Qu, J.; Zhang, J.; Wei, J.; Tao,W.; Air side heat transfer enhancement using radiantly arranged winglets in fin-and-tube heat exchanger, International Journal of Thermal Sciences 156, (2020).

[5]. Salleh, M. F.; Hussein A. M.; Mazlan A.W.; Thermal and hydraulic characteristics of trapezoidal winglet across fin-and-tube heat exchanger (FTHE), Applied Thermal Engineering 149, pp 1379–1393, (2019).

[6]. Song, K.; Toshio T.; ZhongHao C.; Qiang Z.; Heat transfer characteristics of concave and convex curved vortex generators in the channel of plate heat exchanger under laminar flow, International Journal of Thermal Sciences 137, pp 215–228, (2019).

[7]. Wijayanta, A.T.; Istanto, T.; Keishi K.; Akio M.; Heat transfer enhancement of internal flow by inserting punched delta winglet vortex generators with various attack angles, Experimental Thermal Fluid Sciences, 87, pp 141–148, (2017).

[8]. Sinha, A.; Himadri, C.; Ashwin K.I.; Biswas, G.; Enhancement of heat transfer in a fin-tube heat exchanger using rectangular winglet type vortex generators, International Journal of Heat and Mass Transfer, 101, pp 667–681, (2016).

[9]. Aliabadi, M.K.; S. Zangouei,S.; Hormozi, F.; Performance of a plate-fin heat exchanger with vortex-generator channels: 3D-CFD simulation and experimental validation, International Journal of Thermal Sciences 88, pp 180–192, (2015).

[10]. Delac, B.; Trp A.; Lenic, K.; Numerical investigation of heat transfer enhancement in a fin and tubeheat exchanger using vortex generators, International Journal of Heat and Mass Transfer 78, pp 662–669, (2014).

[11]. He, Y.; Chu, P.; Tao, W.; Zhang, Y.; Xie, T.; Analysis of heat transfer and pressure drop for fin-and-tube heat exchangers with rectangular winglettype vortex generators. Applied Thermal Engineering 61, pp 783–770, (2013).

[12]. Versteeg, H.K. and Malalasekera, W. An Introduction to Computational Fluid Dynamics the Finite Volume Method, 1st ed.; Longman Scientific & Technical: London, UK, (1995).

[13]. Samruaisin, P.; Samutpraphut, B.; Wongcharee, K., Eiamsa-ard, S.; Thermo-Hydraulic Performance of Round Tubes Installed with Double V-Shaped Winglet Vortex Generators: Effect of Blockage Ratio, International Journal of Mechanical Engineering and Robotics Research Vol. 9, No. 3, (2020).

[14]. Lu, G. and Zhou, G.; numerical simulation on performance of plane and curve winglet type vortex generator pairs with punched holes, International Journal of Heat and Mass Transfer 102, pp 679–690, (2016).